05,07

Quasistatic remagnetization of a submicron YIG film

© V.D. Poimanov

Bauman Moscow State Technical University,
Moscow, Russia

E-mail: poymanov@bmstu.ru

Received May 24, 2025
Revised July 9, 2025
Accepted July 9, 2025

The results of theoretical calculations indirectly indicate the presence of a single-domain state in a submicron film of the yttrium iron garnet type with a thickness of less than 100 nm, obtained by liquid-phase epitaxy, which is not detected by standard methods due to its small thickness. Unidirectional rotation of the magnetization vector during cyclic remagnetization of such a film is predicted. Within one cycle, four reorientation transitions are detected, two of which occur in a field of the order of the cubic anisotropy field, and the other two - in a field of the order of $4\pi M$.

Keywords: submicron YIG film, single-domain structure, rotational remagnetization, frequency-field dependence, ferromagnetic resonance, liquid-phase epitaxy.

DOI: 10.61011/PSS.2025.07.61870.140-25

1. Introduction

Despite the widespread and detailed study of ferrite garnet films for more than half a century, the number of studies on them has not decreased to date. This is attributable to the great possibilities of their application in devices for transmitting signals using spin waves [1]. As a rule, studies in this field are related to the propagation of magnetodipole waves in various waveguide geometries. Recently, the propagation features related to the modulation of its parameters have been actively studied [2,3].

Iron-Yttrium garnet (YIG) is one of the best materials in the field of spin dynamics in thin magnetic films. Due to its exceptionally low attenuation, it is widely used in experiments on ferromagnetic resonance [4–8]. The domain structure is known to be a significant obstacle to the propagation of spin waves [9]. For microwave devices operating in the field of zero fields, films should have a thickness of less than 100 nm, while samples with a thickness of about a micron are currently used. If the film is not thin enough (more than 100 nm), then its saturated state is required for the waveguide to function, which can be obtained by applying an additional external field and requires equipping the device with a permanent magnet. Therefore, it is advisable to use submicron films (less than 100 nm) in a single-domain state, for which magnetization is not required. At the same time, there is currently no direct observation of the single-domain nature of such films due to their small thickness and its presence can only be assessed indirectly (by studying the response and using FMR data).

Currently, submicron YIG films are obtained mainly by pulsed laser deposition at high temperature. However, in this case, the film is not monocrystalline, which can only be grown by liquid-phase epitaxy from a melt solution followed by etching to the desired thickness [10–14].

The practical application of submicron YIG films is not limited to their use as waveguides. When a rotational magnetic field is applied, such films are used as elements for the magnetometer [15], which registers ultra-weak magnetic fields, and also as the core of the magnetic field converter [16].

In this paper, the remagnetization of a film in a single-domain state with a normal along one of the light axes of cubic anisotropy between its saturation fields is theoretically modeled. The field dependences of the orientation angles of the equilibrium magnetization, the FMR and response curves are obtained. It is shown that the application of a quasi-static external field during a complete magnetization reversal cycle leads to unidirectional irreversible rotation of the magnetization vector. At full pulling of the quasinormal field, two orientational transitions were detected between saturation states.

2. Description of the model

Let us consider a submicron film of the YIG type with a thickness of about 100 nm, which is in a single-domain state (Figure 1). The film is positioned on the substrate so that one of its light axes of the third order [111] is oriented along the normal (axis z). The other two axes x and y are directed respectively along the directions $[11\bar{2}]$ and $[\bar{1}10]$. The directions indicated by the dotted line are projections of three other light bilateral axes of the third order, located in the planes formed by them with a normal at an angle $\theta_0 \approx 70.5^\circ$ to it.

The energy density of the considered structure:

$$W = 4\pi M^2 \frac{\cos^2\theta}{2} - H_c M\Big(\frac{\sin^4\theta}{4} + \frac{\cos^4\theta}{3} + \frac{\sqrt{2}}{3}\sin^3\theta\cos\theta\cos(3\varphi)\Big) - HM\big(\cos\theta\cos\theta_H + \sin\theta\sin\theta_H\cos(\varphi-\varphi_H)\big). \quad (1)$$

Here θ and φ are the polar and azimuthal orientation angles of equilibrium magnetization, θ_H and φ_H are the field applications, M is the saturation magnetization ($4\pi M = 1250$ OE), $H_c = 45$ OE is the cubic anisotropy field. A high-frequency alternating field is applied in the film plane perpendicular to the direction of the quasi-static external field H.

The equilibrium orientation of the magnetization is determined from the equilibrium conditions:

$$W'_\theta = W'_\varphi = 0. \quad (2)$$

It should be noted that the energy density (1) is invariant with respect to the substitution $\theta \to \pi - \theta$, $\varphi \to \varphi \pm \pi$, so in this case all the dependencies for forward and reverse field sweeps between mutually antiparallel saturation states will be symmetric. There are 6 equilibrium orientations of magnetization as follows from the analysis (1), in the absence of an external field

$$\xi_0\colon\ \varphi_0 = 0, \pm\frac{2\pi}{3}, \quad \pi - \xi_0\colon\ \varphi_0 = \pm\frac{\pi}{3}, \pi$$

$\xi_0 \approx \frac{\sqrt{2}}{3}\frac{H_c}{4\pi M} = 1^\circ$ is the polar angle measured from the film plane. The projections of the light axes onto the plane together with the normal form six light planes. During remagnetization in any of these planes, the magnetization does not leave it and there are no orientation transitions.

At values of a strictly normally applied external field greater than $4\pi M - \frac{4}{3}H_c$, the equilibrium magnetization is normal to the film plane. As the external field decreases to zero, the orientation of the magnetization is determined from the equation following from (2):

$$H = 4\pi M + H_c\Big(\cos\theta\Big(1 - \frac{7}{3}\cos^2\theta\Big) + \sqrt{2}\sin\theta\Big(1 - \frac{4}{3}\sin^2\theta\Big)\Big). \quad (3)$$

The dependence of the angle on the external field is shown in Figure 2 [17]. It follows that at $H = -\frac{\sqrt{2}}{3}H_c$, the magnetization vector in the film plane is reoriented from $\varphi_) = 0$ to one of the two states $\varphi_0 = \pm\frac{\pi}{3}$. The magnetization vector rotates in one of these planes to saturation with a further increase in the external field in the direction $\theta_0 = \pi$. In this case, the behavior of the magnetization upon reaching the orientation transition (OT) field is ambiguous. In reality, it is impossible to achieve a strictly normal application, so there is a planar component of the field that can additionally rotate the magnetization in the film plane.

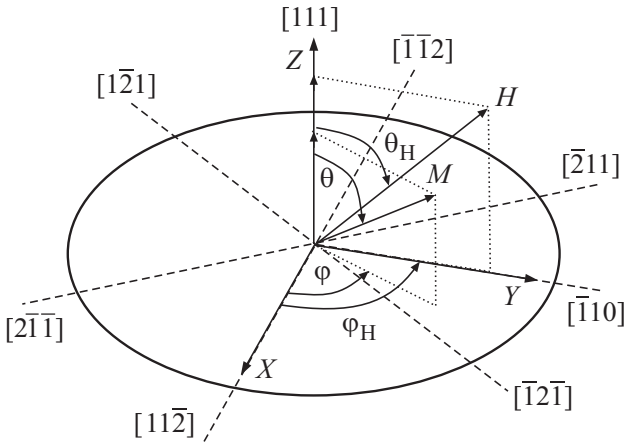

Figure 1. Geometry of structure. The orientation of the light axes is shown. The external field and magnetization with respect to the axes of the selected coordinate system. The figure is taken from Ref. [17].

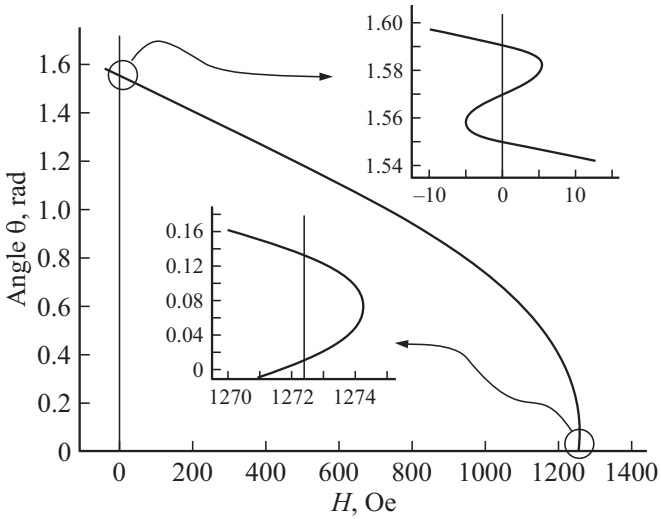

Figure 2. Normal magnetization curve ($\theta_H = 0^\circ$). The figure is taken from Ref. [17].

3. Quasi-normal magnetization reversal

Now let's consider the case of applying a field at angles $\theta_H = 1^\circ$, $\varphi_H = 30^\circ$ with two pulls of its value with reverse ($1300\,\text{OE} \to -1300\,\text{OE}$, „–“) and direct ($-1300\,\text{OE} \to 1300\,\text{OE}$, „+“) orientations. The energy released during the OT is used to excite spin waves in the film, so that the model under consideration works as their generator.

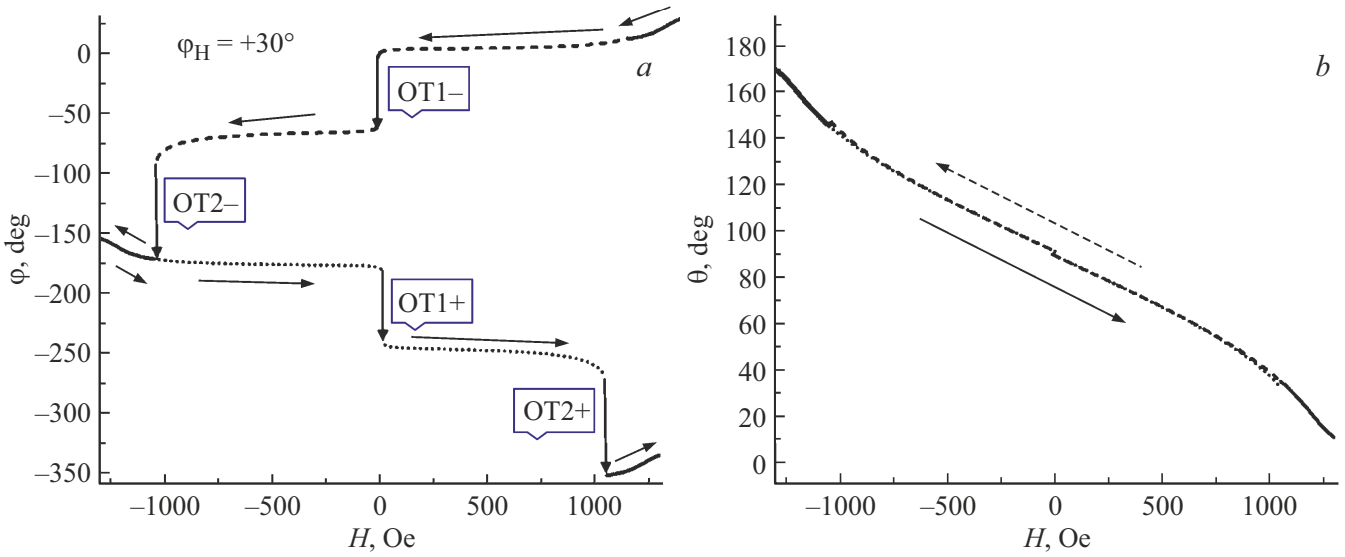

Figure 3. Theoretical dependence of azimuthal (a) and polar (b) angles in case of cyclic remagnetization of a submicron film of the YIG type for $\theta_H = 1°$. $\varphi_H = 30°$. The dashed line indicates the reverse pulling, the dotted line indicates the direct pulling, the solid line indicates the sections without hysteresis.

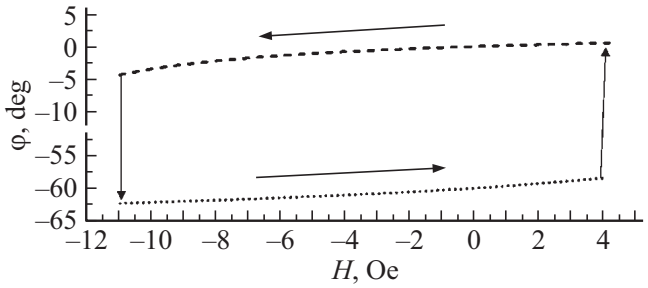

Figure 4. Hysteresis behavior of the azimuthal angle when switching the field near OP1 for $\theta_H = 1°$. $\varphi_H = 30°$.

An analysis of the dependence of the equilibrium azimuthal magnetization angle shows the presence of discontinuities in it associated with OT and loss of stability during both forward and reverse magnetization reversal. For each of them, in addition to the above transition near the zero value of the external field (OP1), there is a transition in a field comparable to the saturation field (OP2). This is due to the intermediate capture of magnetization by another light axis of cubic anisotropy. The polar angle changes relatively smoothly during operation.

As follows from Figure 3, a, during a full cycle (reverse and forward field stretching), the magnetization vector rotates clockwise in the film plane by one revolution.

When switching the external field near OP1, a hysteresis asymmetric behavior of the azimuthal angle is observed, shown in Figure 4.

It should be noted that it makes no sense to talk about hysteresis near OP2. This is due to the fact that at OP1, the external field „pushes“ magnetization through the difficult plane $\varphi = -\frac{\pi}{3}$. If, after OP1, the negative field is reduced modulo, then for the new state of magnetization $\varphi = -\frac{\pi}{3}$ is already a plane with an easy axis, and the plane with the axis $\varphi = 0$ becomes difficult. Since at OP1 the magnetization intersects the film plane, the light and hard planes change roles. In the case of OP2, this does not happen, and the plane $\varphi = -\frac{2\pi}{3}$ is again difficult. The azimuth transition through this plane occurs when a large negative field is applied. Thus, unidirectional rotation becomes possible due to the presence of OP2.

The field dependence of the FMR frequency (Figure 5), constructed for the frequency of a high-frequency field of 700 MHz, has a pronounced asymmetry with respect to the change in the sign of the field during pulling in both directions. This is due to the fact that as the field decreases, the magnetization monotonously orients towards the plane of the nearest light axis. With further remagnetization in the region of negative fields for reorientation in the opposite direction, the magnetization passes through the intermediate light axes. The derivative with respect to the field of y-component of the response to an external high-frequency field of a single amplitude is shown in Figure 6. The maxima of this dependence correspond to the intersection of the frequency-field dependencies in Figure 5 with the straight line $f = 700$ MHz.

Due to the downward shift of the frequency field dependencies in negative fields for $\theta_H = 1°$, the maxima of the derivative of susceptibility are weakly expressed due to the orientation of the equilibrium magnetization in the direction close to the axis y. The highest value of the maximum corresponds to saturation. At the same time, for

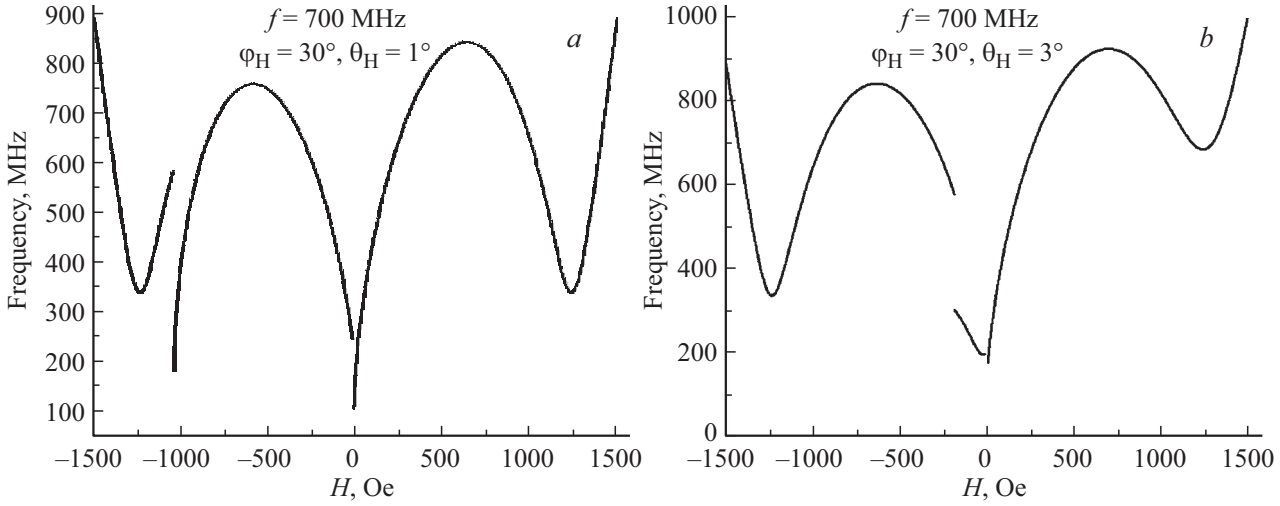

Figure 5. Frequency-field dependence of the homogeneous FMR of the YIG submicron film, corresponding to the reverse pull along the field for $\theta_H = 1^\circ$ (a) and $\theta_H = 3^\circ$ (b). With a direct pull, the graphs are obtained by reflection from the ordinate axis. The discontinuities of the curves correspond to the OT.

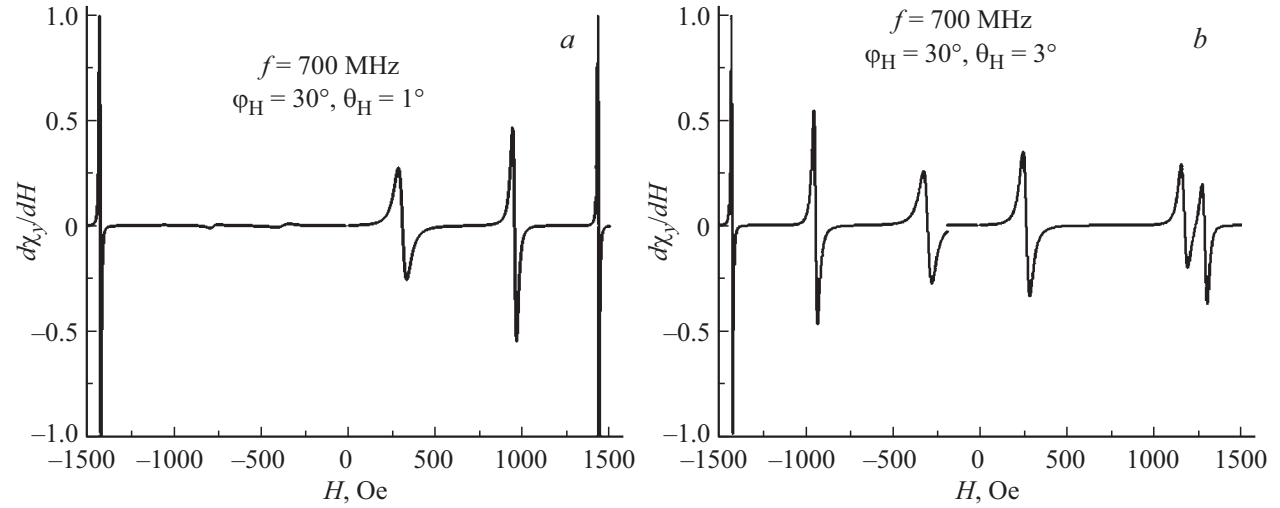

Figure 6. Derivatives of susceptibility along the axis y over the field at a frequency of 700 MHz, corresponding to the graphs in Figure 5.

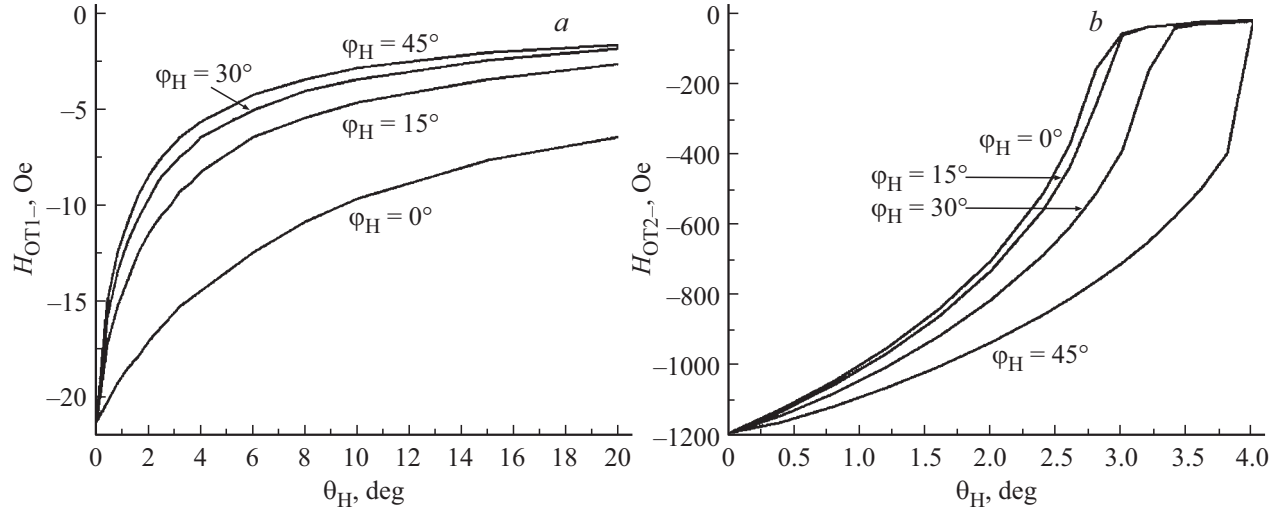

Figure 7. Angular dependencies on θ_H fields OP1- (a) and OP2- (b) for $\varphi_H = 0^\circ$, 15°, 30° and 45°.

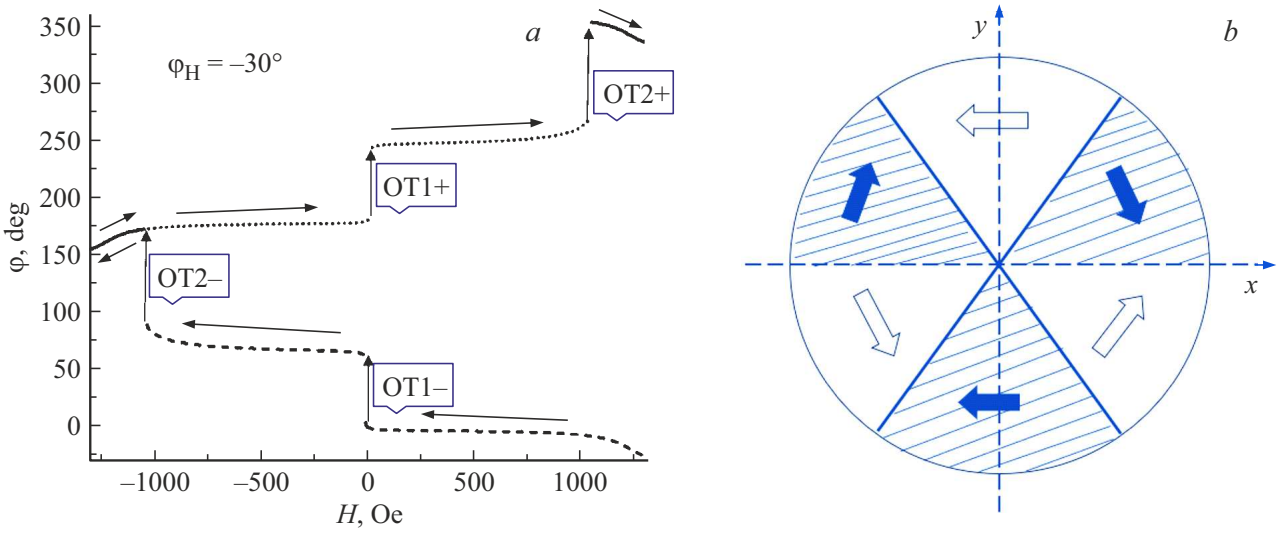

Figure 8. *a* — dependence of the azimuthal angle during magnetization reversal at angles $\theta_H = 1°$. $\varphi_H = 30°$. The dashed line indicates the reverse pulling, the dotted line indicates the direct pulling, the solid line indicates sections without hysteresis. *b* — schematic representation of the direction of rotation of the magnetization vector as a function of the azimuthal angle of application of an external field φ_H quasi-parallel to the positive direction of the axis z.

$\theta_H = 1°$, the amplitude maximum closest to zero exceeds the maximum corresponding to saturation.

Figure 7 shows the dependencies on θ_H fields of OP1 (Figure 6, *a*) and OP2 (Figure 6, *b*) for the values of $\varphi_H = 0°$, 15°, 30° and 45°.

As can be seen from Figure 7, the OP1 field decreases modulo the growth of θ_H. This is due to the fact that this increases the component of the field in the plane that rotates the magnetization. As φ_H increases, the projection of the magnetization to the direction of the external negative field increases, so the OP1 transition field also decreases. On the contrary, for OP2, as φ_H increases to 60°, the projection of the external field on the difficult axis −120° increases with negative magnetization reversal. A component perpendicular to this direction is required to pass through this plane. This explains the modulo increase in the OP2 field with an increase of φ_H.

The application of an external field at an angle $\varphi_H = -30°$ leads to a change in the direction (chirality) of rotation of the magnetization when the external field changes (Figure 7, *a*), which in this case occurs counterclockwise. This is due to the fact that the light axis corresponding to the direction $\varphi = 0$ attracts the magnetization when the field decreases from the saturated state for both positive and negative azimuth angles, so that the magnetizations for these two cases rotate in opposite directions (Figure 8, *b*).

4. Conclusion

In this paper, we simulate the processes of remagnetization of single-domain films by a quasi-normal quasi-static external magnetic field during pulling between states saturated along the direction of the external field. By comparing the experimental dependences of FMR frequencies and theoretical curves, it is possible to establish the orientation of the light axes of the third order in the YIG. Absorption of field energy near its zero value has been detected, which indicates the presence of a reorientation transition near field values of the order of several oersted and is the physical basis for the operation of a small magnetic field sensor. The second transition occurs already in the range of fields comparable to the saturation field. It is shown that, depending on the direction of application of the field in the film plane, unidirectional rotation of the magnetization vector is possible. This effect can be used to design magnetic sensors and spin wave generators, as well as micro-sized microwave devices with non-reciprocal properties.

Appendix. Calculation formulas

The equilibrium orientation of the magnetization is determined from the equilibrium conditions: $W'_\theta = W'_\varphi = 0$.

The frequency of homogeneous FMR

$$\nu_r = \frac{\gamma}{2\pi M} \frac{\sqrt{W''_{\theta\theta} W''_{\varphi\varphi} - (W''_{\theta\varphi})^2}}{\sin\theta},$$

where θ is the equilibrium angle, $\gamma = 1.76 \cdot 10^7$ 1/OE · s gyromagnetic ratio.

Spherical components of the susceptibility tensor at frequency f:

$$\hat{\chi} = \begin{pmatrix} \chi_{\theta\theta} & \chi_{\theta\psi} \\ \chi_{\psi\theta} & \chi_{\psi\psi} \end{pmatrix} = \frac{\begin{pmatrix} W''_{\varphi\varphi} - i\alpha f \dfrac{2\pi M}{\gamma} \sin^2\theta & -\sin\theta(W''_{\theta\varphi} + i\alpha f \dfrac{2\pi M}{\gamma} \sin\theta) \\ -\sin\theta(W''_{\varphi\theta} - i\alpha f \dfrac{2\pi M}{\gamma} \sin\theta) & \sin^2\theta(W''_{\theta\theta} - i\alpha f) \end{pmatrix}}{W''_{\theta\theta}W''_{\varphi\varphi} - (W''_{\theta\varphi})^2 - i\dfrac{2\pi M}{\gamma}\alpha f(W''_{\theta\theta}\sin^2\theta + W''_{\varphi\varphi})},$$

where α is the Hilbert decay constant.

The magnitude of the response to a high-frequency field of a single amplitude along the axes x and y:

$$\chi_x = (\chi_{\theta\theta}\cos\theta\cos\varphi - \chi_{\psi\theta}\sin\varphi)\cos(\varphi - \varphi_h)\cos\theta + (\chi_{\theta\psi}\cos\theta\cos\varphi - \chi_{\psi\psi}\sin\varphi)\sin(\varphi - \varphi_h),$$

$$\chi_y = (\chi_{\theta\theta}\cos\theta\sin\varphi - \chi_{\psi\theta}\cos\varphi)\cos(\varphi - \varphi_h)\cos\theta + (\chi_{\theta\psi}\cos\theta\sin\varphi + \chi_{\psi\psi}\cos\varphi)\sin(\varphi - \varphi_h).$$

Conflict of interest

The author declares that he has no conflict of interest.

References

[1] S.O. Demokritov. Spin Wave Confinement: Propagating waves, Pan Stanford Publishing: 2nd edition (2017), p. 448.
[2] V.D. Poimanov, V.V. Kruglyak. ZhETF **161**, *5*, 720–736 (2022). (in Russian).
[3] A.A. Martyshkin, E.N. Beginin, A.V. Sadovnikov. AIP Advances **11**, 035024 (2021).
[4] N.S. Akulov. Ferromagnetizm. GITTL, M., L. (1939). p. 186. (in Russian).
[5] A.G. Gurevich. Magnitnyi rezonans v ferritakh i antiferomagnetikakh Nauka, M. (1973). 593 p. (in Russian).
[6] T. Liu, H. Chang, V. Vlamnick, Y. Sun, M. Kabatek, A. Hoffmann, L. Deng, M. Wu. J. Appl. Phys. **115**, 17A501 (2014).
[7] Y. Sun, Y.-Y. Song, H. Chang, M. Kabatek, M. Jantz, W. Schneider, M. Wu, H. Schultheiss, A. Hoffmann. Appl. Phys. Lett. **101**, 152405 (2012).
[8] Y. Sun, H. Chang, M. Kabatek, Y.-Y. Song, Z. Wang, M. Jantz, W. Schneider, M. Wu, E. Montoya, B. Kardasz, B. Heinrich, S.G.E. Velthuis, H. Schulthheiss, A. Hoffmann. Phys. Rev. Lett. **111**, 106601 (2013).
[9] Y.M. Nikolaenko, N.I. Mezin, V.V. Kononenko, N.B. Efros. Fizika i tekhnika vysokikh davleniy **27**, *4*, 101–109 (2017). (in Russian).
[10] E.I. Nikolaev, I.A. Krasin. Kristallografiya, **33**, *2*, 478 (1988). (in Russian).
[11] P. Görnert, R. Hergt, E. Sinn, M. Wendt, B. Keszei, J. Vandlik. J. Cryst. Growth **87**, 331 (1988).
[12] H. Wei, W. Wang. IEEE T. Magn. **20**, 1222 (1984).
[13] J. Čermák, A. Abrahám, T. Fabián, P. Kaboš, P. Hyben. JMMM **83**, 427 (1990).
[14] D. Yong Choi, S. Jin Chung. J. Cryst. Growth **191**, 754 (1998).
[15] P.M. Vetoshko, N.A. Gusev, D.A. Chepurnova, E.V. Samoilova, I.I. Seroka, I.M. Seroka, A.K. Zvezdin, A.A. Korotaeva, V.I. Belotelov. Pis'ma v ZhTF **42**, *16*, 64 (2016). (in Russian).
[16] S.B. Ubizskii. JMMM **219**, 127 (2000).
[17] V.F. Shkar, E.I. Nikolaev, V.N. Sayapin, V.D. Poymanov. FTT **46**, *6*, 1043–1050 (2004). (in Russian).
[18] V.F. Shkar, V.N. Varyukhin. Pisma v ZhETF **88**, 311 (2008). (in Russian).
[19] V.F. Shkar, V.N. Varyukhin. Pisma v ZhETF **92**, 375 (2010). (in Russian).
[20] V.D. Poimanov, V.F. Shkar, Y.I. Nepochatykh, V. Sampath, V.V. Koledov, V.G. Shavrov. JMMM **443**, 319 (2017).

Translated by A.Akhtyamov